Construction of a New Artificial Biomineralization System

Takashi Iwatsubo,* Kimio Sumaru, Toshiyuki Kanamori, Toshio Shinbo, and Tomohiko Yamaguchi

Research Center of Advanced Bionics and Nanotechnology Research Institute, National Institute of Advanced Industrial Science and Technology, Central 5, 1-1-1 Higashi, Tsukuba, Ibaraki 305-8565, Japan

Received June 27, 2005; Revised Manuscript Received October 16, 2005

Hydroxyapatite (HAP) was mineralized in poly(vinyl alcohol) (PVA)/poly(acrylic acid) (PAA) complex hydrogel immersed in a salt solution containing PAA. The transparent HAP/polymer composite swelled in water depending on the HAP content; high HAP content gave small swelling and vice versa. The HAP content reached about 80 wt % at most. Observation of the cross section of the composite by energy-dispersive analysis of X-ray (EDAX) revealed that the composite consisted of two phases, i.e., a hard HAP-rich phase and a soft polymer-rich phase. In the HAP-rich phase, the space inside the hydrogel was occupied by HAP, while HAP was not mineralized in the polymer-rich phase. The nucleation seemed to take place, at first, at the middle depth of the hydrogel where the HAP-rich phase was formed. The HAP-rich phase grew its size toward the surface of the hydrogel at the cost of the polymer-rich phase. The presence of phosphorus, P, in the polymer-rich phase indicated the adsorption of HPO_4^{2-} on the polymer chain of the hydrogel via hydrogen bonding, accompanied with Ca^{2+} because of electrostatic constraints. This adsorption of ions in addition to Donnan distribution of ions leads to the formation of a hypercomplex that can be regarded as a precursor of the HAP-rich phase. The change of the hypercomplex into the HAP-rich phase is discontinuous and hence concluded as a phase transition. By comparison of our mineralization system with the biomineralization system of HAP and $CaCO_3$, the physicochemical mechanism of the mineralization process in the present system was found to be similar to that in biological systems. In this sense, we termed the present system an artificial biomineralization system.

Introduction

Both HAP and $CaCO_3$ are brittle biominerals by themselves; however, when combined with organic polymers in biological processes (biomineralization), the resulting hybrid material changes into a biocompatible material overcoming the intrinsic brittleness. The vertebrate bone as a composite of HAP/polymer, and the exoskeletons of corals, sea urchins, and crustaceans as composites of $CaCO_3$/polymer are typical familiar examples.

In many biological systems, ionic polymers are known to be concerned in biomineralization. An osteoblast produces acidic proteins such as osteonectin (ON), osteopontin (OPN), osteocalcin (OC), and bone sialoprotein (BSP). Bone composed of collagen and HAP also contains OC and BSP. In the counter perfusion of a $CaCl_2$ solution and a sodium phosphate solution separated by an agarose gel membrane in which acidic protein was incorporated, the $Ca + PO_4$ content inside the gel increased compared with a negative control (no added protein) even though calcium and phosphate concentrations were below the threshold of spontaneous precipitation of HAP. From this nucleation assay, BSP were revealed to act as nucleators of HAP.[1] In the autotitration of aqueous solutions that contained $CaCl_2$, sodium phosphate, and acidic protein to be maintained at pH 7.4 by addition of 50 mM NaOH, OC and OPN were found to act as inhibitors of HAP formation in a solution phase.[1] The exoskeleton of crustaceans is composed of chitin, $CaCO_3$, and acidic proteins. When incorporated in amylose resin beads, the acidic protein crustcalcin (CCN) extracted from the exoskeleton of penaeid prawn, *Penaeus japonicus*, acts as a nucleator of $CaCO_3$ to allow the formation of $CaCO_3$ particles.[2] The acidic protein, which was extracted from the exoskeleton of crayfish, *Procambarus clarkia*, and named CAP-1, acts as an inhibitor of $CaCO_3$ formation in a solution phase and has an adsorption ability on chitin.[3] The CAP-1 adsorbed on chitin was found to act as a nucleator of $CaCO_3$.[4] In this way, the ionic polymers tend to be an inhibitor in a solution phase while a nucleator in a fixed phase. Nonetheless, the mechanism of how they act as inhibitors or nucleators depending on the conditions in which they exist is still unknown. The knowledge of how polymers and salt ions can work cooperatively in biomineralization is also lacking. Thus the physicochemical mechanism of biomineralization has not yet been solved clearly.

Needless to say, mixing the constituent salt solutions of excess concentrations at appropriate pH can easily form biominerals. The difficulty is how to combine biominerals with organic polymers and to construct a 3-dimensional composite. If biominerals can be synthetically deposited on polymers, the composite will be used as a biocompatible or new hybrid material. For this purpose, the synthesis of composites between biominerals and organic polymers has been investigated extensively.[5−12] The authors reported in a previous paper that the HAP/polymer composite was manufactured by mineralizing HAP in PVA/PAA hydrogel immersed in a salt solution containing PAA.[13] The mineralized substance was identified as HAP from the powder X-ray diffraction peak and the molar ratio of [Ca]/[P] determined by inductively coupled plasma atomic emission spectroscopy (ICP). The HAP content in the composite reached more than 70% in weight. From the broadening of the X-ray diffraction peaks, the crystallinity of HAP was estimated to be low.

* To whom correspondence should be addressed. Phone: +81-29-861-4758. Fax: +81-29-861-4651. E-mail: t-iwatsubo@aist.go.jp.

10.1021/bm0504476 CCC: $33.50
Published on Web 12/10/2005

Table 1. Constituent Polymers in Several Biomineralization Systems

system	ionic polymer and its function				
biomineral/neutral polymer	anionic	cationic	adsorbed in polymer matrix	in aq soln	ref
bone of pig calvaria					
$Ca_{10}(PO_4)_6(OH)_2$/collagen	osteonectin (ON)				1
	osteopontin (OPN)			inhibitor	1
	osteocalcin (OC)			inhibitor	1
	bone sialoprotein (BSP)		nucleator		1
exoskeleton of penaeid prawn					
$CaCO_3$/chitin	crustcalcin (CCN)		nucleator		2
exoskeleton of crayfish					
$CaCO_3$/chitin	CAP-1		nucleator	inhibitor	4/3
cell wall of diatom					
SiO_2/glycoprotein					16
		silaffin-1		inhibitor?	17
	silaffin-2				18
artificial biomineralization					
$Ca_{10}(PO_4)_6(OH)_2$/PVA	PAA		nucleator	inhibitor	this work

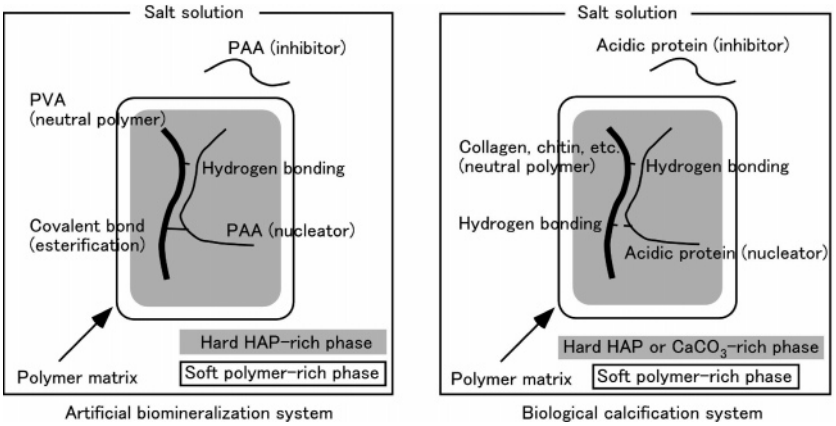

Figure 1. Schematic representation of the artificial biomineralization system (left) as an analogue of the biological calcification system (right).

In the present paper HAP mineralization in PVA/PAA hydrogel is further examined. The weight increase of the composite in the mineralization process and the swelling degree of the obtained composite in water are measured to make clear the HAP mineralization process. Furthermore, a part of the HAP mineralization mechanism is revealed by the EDAX method. We also point out that our mineralization system is analogous to biological mineralization systems and discuss the physicochemical mechanism of biomineralization.

System Design

There is an attractive interaction between the polymer chains of PVA and PAA through hydrogen bonding where the −OH of PVA acts as a proton donor and the $-COO^-$ of PAA acts as a proton acceptor.[14] This hydrogen bonding has a capability to immobilize PAA within the polymer matrix. In our system, partial esterification will be solely introduced to build a hydrogel having enough strength for the measurement of swelling degree. The PAA in the salt solution acts as an inhibitor of nucleation,[9−13,15] while the PAA immobilized in the hydrogel is thought to induce the nucleation of HAP.[13] The bimodal function of these conflicting effects of PAA may enable the mineralization of HAP in the interior of the hydrogel. Hereupon we encounter the analogy between our mineralization system and a hard tissue formation system in biomineralization. The neutral polymer PVA can be an analogue of collagen or chitin, and the acidic polymer PAA can be an analogue of acidic proteins found in biological systems (Table 1). Furthermore, the complex formation between PVA and PAA through hydrogen bonding can be analogous to the complex formation[4] between chitin and acidic protein CAP-1 through hydrogen bonding. Most probably, collagen also has the ability of hydrogen bonding with acidic proteins via its abundant hydroxyproline residues. Then we can go ahead along these analogies to outline the scenario of hard tissue formation in biomineralization, as illustrated in Figure 1, for the case of calcification. Neutral polymer collagen or chitin that has −OH or −NH, as a proton donor, and acidic proteins that have, for example, $-COO^-$ on aspartate residues[15] as a proton acceptor, form together a polymer matrix by hydrogen bonding. These acidic proteins bound in the matrix act as nucleators, whereas the acidic proteins that do not participate in matrix formation act as inhibitors of nucleation to maintain the salt concentration at an elevated level in the external solution. If such a system is constructed under appropriate conditions such as temperature, pH, concentrations etc., the biomineral of our concern may be formed within the polymer matrix.

Experimental Section

Materials. PVA (degree of polymerization, ca. 2000), calcium chloride dihydrate ($CaCl_2 \cdot 2H_2O$), sodium chloride (NaCl), diammonium

hydrogen phosphate ($(NH_4)_2HPO_4$), and a solution of 1 M tris(hydroxymethyl)aminomethane hydrochloride (Tris−HCl) buffer were purchased from Wako Pure Chemical Industries, Ltd. (Osaka, Japan). Two types of PAA, the molecular weight (M_w) of ca. 2000 Da and the average M_w of 250 000 Da, were purchased from Sigma-Aldrich Corporation (St. Louis, MO).

Mineralization Conditions. To prepare a PVA/PAA complex film, aqueous solutions containing 1 wt % of PVA and 1 wt % of PAA (M_w 250 000 Da) were mixed with a weight ratio of PVA/PAA at 1:1. The mixed solution was stirred for 2 h at room temperature to obtain a homogeneous solution. The solution was then cast onto polystyrene Petri dishes, and water was allowed to evaporate at room temperature for almost 1 week. Finally, the films were dried in vacuum at room temperature for 1 day. The resulting films were easily peeled off from the dishes and were about 30 μm thick and transparent, indicating the good miscibility of PVA and PAA. The PVA/PAA complex films were heated at 110 °C in a vacuum oven for 1 h to introduce cross-links between the polymer chains of PVA and PAA by esterification.[13,19] Circular pieces with 1 cm radius were cut out of the film for mineralization experiments.

The salt solution was 5 mM $CaCl_2$ and 3 mM $(NH_4)_2HPO_4$, both as the source ions for HAP, 0.139 mM in the repeating unit of PAA (M_w 2000 Da) as an inhibitor of crystallization in the outer solution phase, and 140 mM NaCl. The pH of the solution was regulated at 7.45 by Tris−HCl buffer. The NaCl concentration and pH were chosen as similar to those of body fluid.[20] The high concentrations of source ions in the solution were maintained by the existence of PAA, because the solution without PAA generated precipitation, whereas our solution kept its transparency for more than 2 weeks. In this sense PAA certainly acts as an inhibitor of nucleation in our system. But the solution containing 6 mM $CaCl_2$ and 3.6 mM $(NH_4)_2HPO_4$ with 140 mM NaCl and pH = 7.45 generated precipitation. Hence, our salt solution exists slightly below the precipitation threshold. The polymer film was soaked in a 200 mL salt solution thermostated at 30 °C. The solution was renewed every 24 h. Using the soaking processes with different time intervals for different source films, we determined the time course of the weight increase of the inorganic component in the composite film.

Evaluation of Mineralized Materials. After an appropriate time interval, the soaked film was taken out from the solution and then rinsed three times in pure water for 10 min each to remove residual soluble ions inside the sample. The wt % of inorganic constituents in the obtained organic/inorganic composite, W, was calculated as $W = 100\text{-}(M - M_0)/M$, where M_0 and M are the weights of the sample dried in vacuum for 24 h before and after the mineralization process, respectively. The swelling degree of the composite, r, was determined as follows. The vacuum-dried organic/inorganic composite was soaked and equilibrated in pure water at 30 °C for 1 h. The swollen composite taken out of water was immediately wrapped with filter paper and was centrifuged in order to remove the remaining water on the swollen composite surface.[21,22] The centrifuge was run at 2500 rpm for less than 1 min, depending on the value of W. Then the weight of the swollen composite, M', was measured, and the swelling degree r was calculated as $r = 100(M' - M)/M$.

The composites frozen by liquid nitrogen were cut and carbon-coated to obtain about 15 nm thickness of carbon surface layer. Their cross sections were observed by scanning electron microscopy (SEM). The distribution profiles of elements C, O, Ca, and P were analyzed by energy-dispersive analysis of X-ray (EDAX).

Results and Discussion

Time Course of Mineralization. The PVA/PAA film swelled to be hydrogel in the salt solution. Throughout the mineralization process, all composites maintained their transparency. The wt % of inorganic content in the organic/inorganic composite increased with mineralization time T and reached the plateau of about W = 78% (Figure 2). This saturation means that mineralization has been terminated and the system reached equilibrium. The swelling degree of the composite, r, was initially about 200% (i.e., the swelling degree of the PVA/PAA film) and then decreased as mineralization proceeded down to about 10% after 200 h. These observations indicate that the inorganic component increases the volume by excluding the salt solution from the hydrogel, and after 200 h, the space between the polymer chains should be practically occupied by the inorganic component. At the early stage, the composite of W = 36.7% was flexible in the wet state. But the composites of W > 41.5% lost the flexibility and became hard in the wet state. This hard component had been identified as HAP.[13]

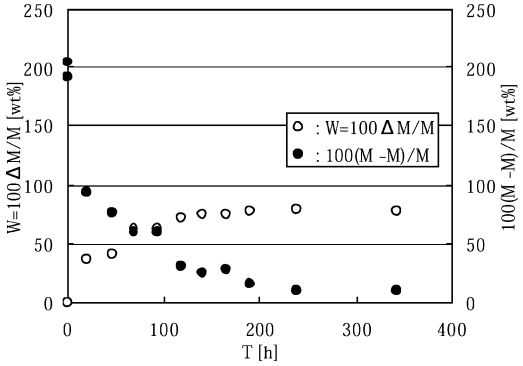

Figure 2. Weight percent of inorganic constituents in the obtained organic/inorganic composite, W, and the swelling degree of composite, r, are plotted against mineralization time T. $\Delta M = M - M_0$. The amount of inorganic components increases by excluding water up to fulfill the space between the polymer chains of swollen hydrogel.

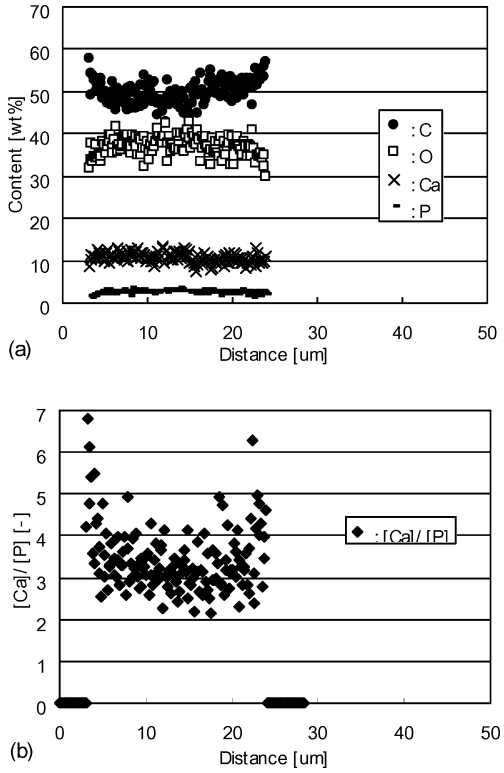

Figure 3. Concentration profiles of C, O, Ca, and P (a) and [Ca]/[P] profile (b) in the cross section of the composite with W = 36.7%. Quantitative line analysis is represented along the thickness of the composite from the surface to the opposite side of surface.

SEM−EDAX Observation. Figures 3a−6a demonstrate the concentration profiles of C, O, Ca, and P in wt % along the thickness of the composite hydrogel of W = 36.7, 41.5, 62.2, and 78.4%, respectively, determined by quantitative line analysis

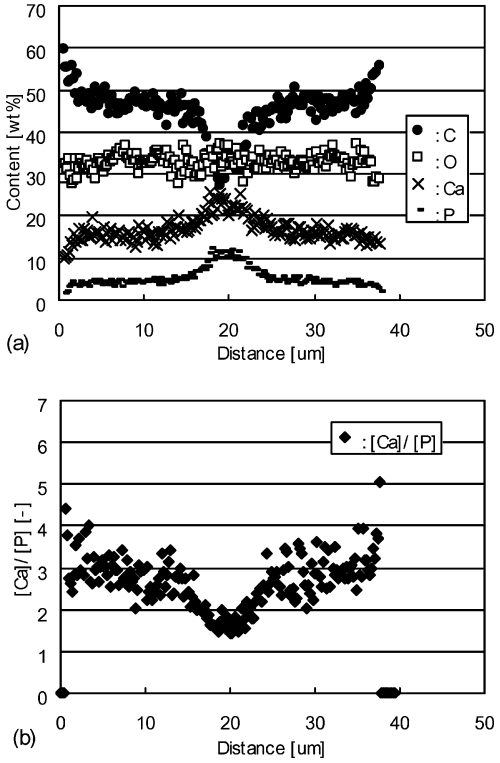

Figure 4. Concentration profiles of C, O, Ca, and P (a) and [Ca]/[P] profile (b) in the cross section of the composite with $W = 41.5\%$. Quantitative line analysis is represented along the thickness of the composite from the surface to the opposite side of surface.

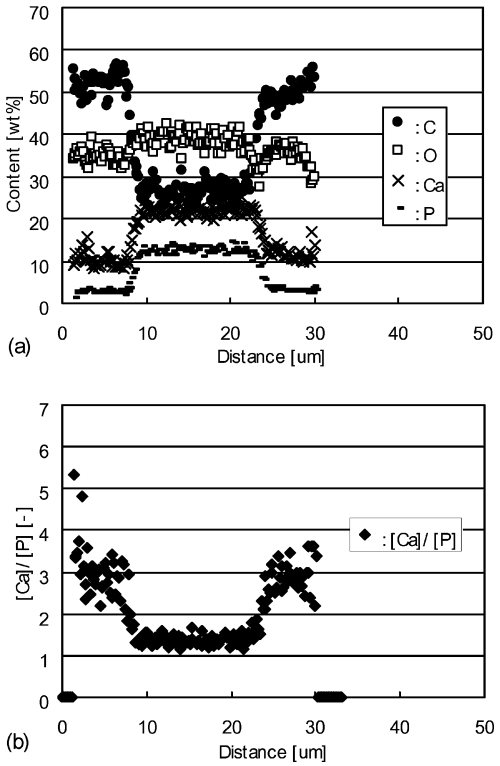

Figure 5. Concentration profiles of C, O, Ca, and P (a) and [Ca]/[P] profile (b) in the cross section of the composite with $W = 62.2\%$. Quantitative line analysis is represented along the thickness of the composite from the surface to the opposite side of surface.

of EDAX. The sum of the amounts of these four elements is normalized as 100%. The molar ratio, [Ca]/[P], was calculated from Figures 3a−6a and is shown in Figures 3b−6b. In the early profiles illustrated in Figure 3a ($W = 36.7\%$), the existing

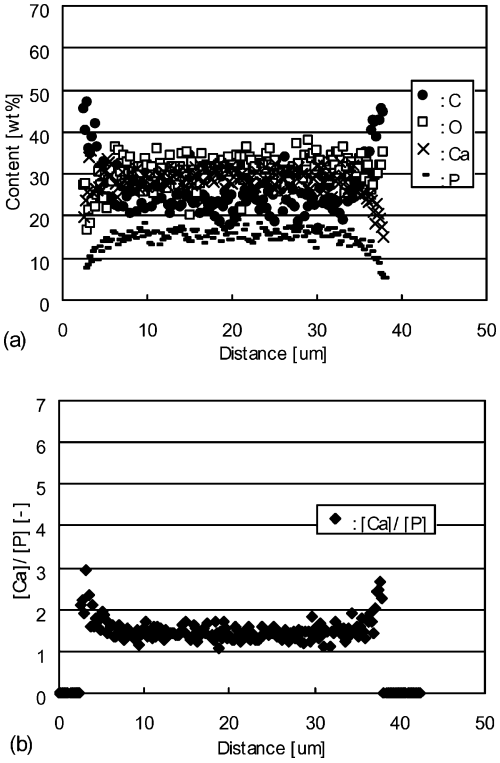

Figure 6. Concentration profiles of C, O, Ca, and P (a) and [Ca]/[P] profile (b) in the cross section of the composite with $W = 78.4\%$. Quantitative line analysis is represented along the thickness of the composite from the surface to the opposite side of surface.

Ca and P will not be those of HAP because [Ca]/[P] = 3 as can be seen in Figure 3b is different from that of HAP ([Ca]/[P] = 1.67). These elements will be therefore those of ions adsorbed on the polymer chain. The flexibility of this composite in the wet state supports this presumption. At the next stage, shown in Figure 4a ($W = 41.5\%$), C decreases while Ca and P increase at the middle of the hydrogel. This phenomenon can be regarded as the mineralization of HAP, because the ratio [Ca]/[P] (= 1.5) is close to the value of 1.67 for HAP, as can be seen in Figure 4b. Thus, the formation of HAP was found to take place, at first, at the middle depth of the hydrogel. The middle of the composite ($W = 62.2\%$) then turns to be the HAP-rich phase where the space between the polymer chains is occupied with HAP, because the concentrations of inorganic elements reach constant levels as shown in Figure 5, parts a and b. The peripheral portion surrounding the HAP-rich phase still remains as the polymer-rich phase where mineralization of HAP has not occurred yet. As time proceeds, the front of the HAP-rich phase moves toward the surface at the cost of the polymer-rich phase. Needless to say, it is the polymer-rich phase that holds water by swelling and mainly contributes to the swelling degree of the composite, *r*, in Figure 2. In the composite of $W = 78.4\%$ that corresponds to the saturated level of mineralization in Figure 2, the HAP-rich phase has not reached the surface yet and the surface still seems to be composed of the polymer-rich phase. The results of element mapping at the stage of $W = 41.5\%$ are shown in Figure 7. In Figure 7a that is an SEM image taken in EDAX, the spindle-shaped portion at the middle of the cross section corresponds to the HAP-rich phase. In the HAP-rich phase, the C content is lower while the Ca and the P contents are higher than those in the peripheral polymer-rich phase as shown in Figure 7, parts b, c, and d, respectively.

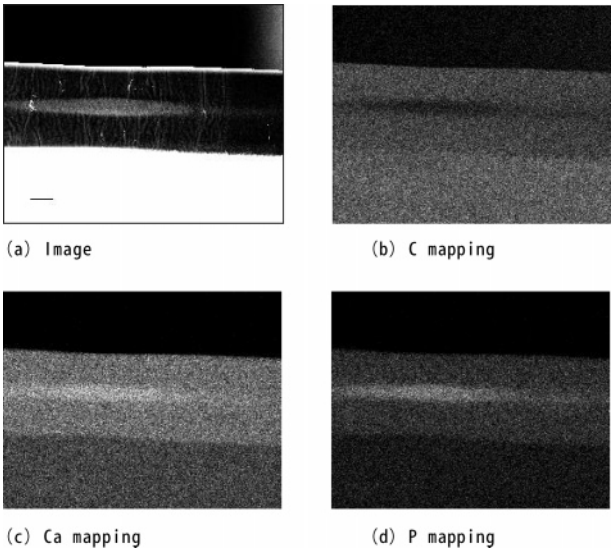

Figure 7. SEM image of cross section (a) and element mappings of C (b), Ca (c), and P (d) at an early stage of the mineralization process. Scale bar, 10 μm.

Discussion

Now we consider the mineralization mechanism of HAP in the PVA/PAA hydrogel. The following discussion will help to understand the natural biomineralization system.

The inhibitory function of PAA and acidic proteins has its origin in the electrostatic potential effect of a dilute polyelectrolyte that decreases the local activity product of ions in an aqueous solution.[23] This effect to decrease the local activity product can be exerted when the polyelectrolyte is dissociated. Therefore, the pH of a salt solution containing acidic protein as an inhibitor should be alkaline, while the pH of a salt solution that contains cationic polymer should be acidic.

Next we discuss the nucleation function of PAA incorporated in polymer matrix. Since phosphoric acid takes the dominant form of HPO_4^{2-} at pH = 7.5,[20] the element P in the polymer-rich phase should be in the form of HPO_4^{2-} that adsorbed on the polymer chains of the hydrogel. This adsorption will be caused by hydrogen bonding also. One example of hydrogen bonding formed by HPO_4^{2-} is given by phosphate-binding protein (PBP) that captures one HPO_4^{2-} entirely by multiple hydrogen bondings[24] where the $-$OH of HPO_4^{2-} donates a proton to the $-COO^-$ of the aspartic acid residue of PBP and the other oxygen atoms of HPO_4^{2-} accept protons from the $-$OH and the $-$NH on PBP. In our system, the $-$OH of HPO_4^{2-} will be a proton donor to the $-COO^-$ of PAA and the other oxygen atoms of HPO_4^{2-} will be proton acceptors from the $-$OH of PVA as illustrated in Figure 8a. When this adsorption of HPO_4^{2-} occurs, Ca^{2+} can be concomitantly absorbed within the polymer matrix by electrostatic interaction with HPO_4^{2-}. In addition to this adsorption of HPO_4^{2-} and absorption of Ca^{2+}, these ionic species can be taken into the polymer matrix by Donnan distribution caused by the electrostatic effect of the $-COO^-$ of PAA. Consequently, a hypercomplex of Ca^{2+}(PVA/HPO_4^{2-}/PAACa) can be formed. This will correspond to the polymer-rich phase observed in the EDAX analysis. The two-phase structure of the composite (Figures 5 and 7) indicates that the change of the polymer-rich phase into the HAP-rich phase is discontinuous and therefore should be regarded as a phase transition. The hypercomplex containing excess ions turns to be unstable under our experimental condition and undergoes

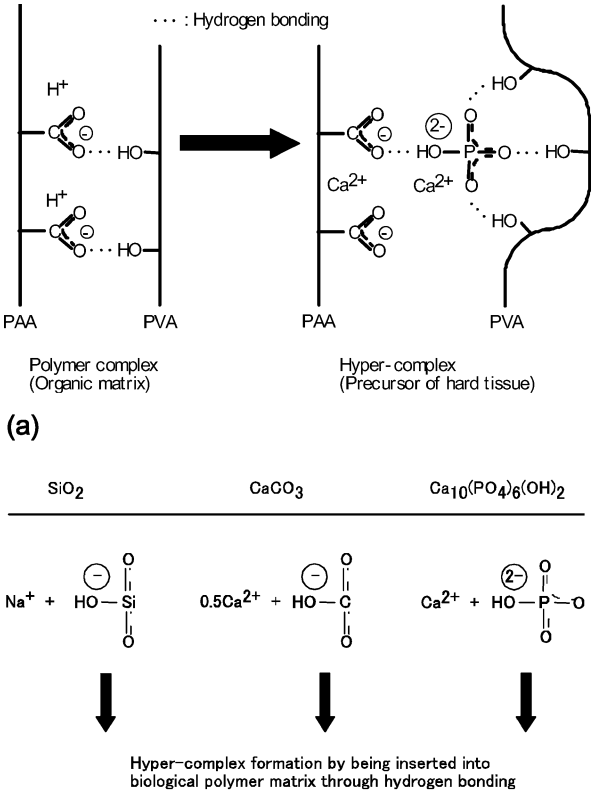

Figure 8. Schematic illustration of hypercomplex formation (right) via the polymer complex (left) in the present system (a) and monoprotonic acids that can be adsorbed by hydrogen bonding on a biological polymer matrix (b). The hypercomplex changes into hard tissue by phase transition.

phase transition accompanying the hydrolysis of

$$5Ca^{2+} + 3HPO_4^{2-} + H_2O \rightarrow Ca_5(PO_4)_3(OH) + 4H^+$$

This scenario of the phase transition of the hypercomplex explains the origin of the nucleation function of PAA or acidic proteins within the hydrogel.

This mechanism can be applied to the biomineralization of $CaCO_3$ and SiO_2 as well. Bicarbonate ion is known to form strong hydrogen bonding in $KHCO_3$ and $NaHCO_3$ with an O$-$H$\cdots$O distance of approximately 2.6 Å.[25] Hence, it can be supposed that, in the case of biomineralization of $CaCO_3$, HCO_3^- will be adsorbed on the polymer matrix in a similar way to HPO_4^{2-} by hydrogen bonding (the $-$OH of HCO_3^- is a proton donor and the other oxygen atoms of HCO_3^- are proton acceptors) to form a precursor that can be converted into $CaCO_3$-containing hard tissue by phase transition accompanying the hydrolysis of

$$Ca^{2+} + HCO_3^- \rightarrow CaCO_3 + H^+$$

In the case of biomineralization of SiO_2 in diatoms, the hydrogen bonding between silicic acid and the polymer matrix had been proposed.[26] On the analogy of the previous two kinds of biominerals, $HSiO_3^-$ that is the anionic constituent of Na_2SiO_3 will be adsorbed on the polymer matrix by hydrogen bonding (the $-$OH of $HSiO_3^-$ is a proton donor and the other oxygen atoms of $HSiO_3^-$ are proton acceptors). Nucleation of hard tissue would then take place accompanying the dehydration of

$$HSiO_3^- \rightarrow SiO_2 + OH^-$$

Apparently this reaction can proceed in acidic condition, where silaffin-1 can be dissociated. Therefore mobile silaffin-1 will have an inhibitory effect on the mineralization of SiO_2 in the solution surrounding the polymer matrix in which SiO_2 is expected to be mineralized. In this way, the cationic polymer silaffin-1 found in a cell wall of a diatom[17] may act as an inhibitor of SiO_2 formation if it exists in the solution surrounding the polymer matrix and the pH of the solution is acidic (Table 1).

Thus, we can extract a universality hidden in different biomineralization systems: In the pH-controlled salt solution, polyelectrolyte dissociates and therefore acts as an inhibitor of nucleation in the solution phase. The dissolving anionic species that is one of the source materials of the biomineral has a common structure of a monoprotonic acid that can be adsorbed on the polymer matrix through hydrogen bonding (Figure 8b). This adsorption leads to the formation of a hypercomplex that can be regarded as a precursor of hard tissue. The hypercomplex (polymer-rich phase) discontinuously changes into the biomineral-rich phase (organic/inorganic solid solution) by a new type of phase transition accompanying hydrolysis (HAP and $CaCO_3$) or dehydration (SiO_2).

Conclusion

We have succeeded in constructing a new artificial biomineralization system where hydroxyapatite (HAP) was mineralized within the PVA/PAA polymer matrix that was built by hydrogen bonding. Through the consideration of this artificial biomineralization system, a part of the physicochemical mechanism of biomineralization can be estimated. In the pH-controlled salt solution, polyelectrolyte polymer acts as an inhibitor of nucleation. We point out that the dissolving anionic species that is one of the source materials of the biomineral has a common structure of a monoprotonic acid that can be adsorbed on the polymer matrix of the hydrogel by hydrogen bonding. This adsorption leads to the recombination of polymer matrix into a hypercomplex that can be regarded as a precursor of hard tissue. The change of the hypercomplex into hard tissue should be regarded as phase transition because of its discontinuity. In an artificial biomineralization system, we can change or control the size and shape of the matrix, time for mineralization, species of polymers, and other factors. Further information about biomineralization will be brought about through the investigation of the artificial biomineralization system to establish a unified mechanism of hard tissue formation.

Acknowledgment. We thank Dr. Horiuchi, Dr. Kihara, Dr. Yokoyama, and Dr. Oyane, who kindly helped us operate the EDAX apparatus. We gratefully acknowledge the financial support provided by the Grant-in-Aid for Scientific Research of the Ministry of Education, Culture, Sports, Science, and Technology (MEXT) of Japan, (B-17350113; 2005).

References and Notes

(1) Hunter, G. K.; Hauschka, P. V.; Poole, A. R.; Rosenberg, L. C.; Goldberg, H. A. *Biochem. J.* **1996**, *317*, 59.
(2) Endo, H.; Takagi, Y.; Ozaki, N.; Kogure, T.; Watanabe, T. *Biochem. J.* **2004**, *384*, 159.
(3) Inoue, H.; Ozaki, N.; Nagasawa, H. *Biosci. Biotechnol. Biochem.* **2001**, *65* (8), 1840.
(4) Sugawara, A.; Kato, T.; Inoue, H.; Nagasawa, H. *Polym. Prepr., Jpn* **2004**, *53* (2), 2Q10.
(5) Taguchi, T.; Kishida, A.; Akashi, M. *Chem. Lett.* **1998**, *8*, 711.
(6) Stupp, S. I.; Ciegler, G. W. *J. Biomed. Mater. Res.* **1992**, *26*, 169.
(7) Kikuchi, M.; Itoh, S.; Ichinose, S.; Shinomiya, K.; Tanaka, J. *Biomaterials* **2001**, *22*, 1705.
(8) Tanahashi, M.; Yao, T.; Kokubo, T.; Minoda, M.; Miyamoto, T.; Nakamura, T.; Yamamoto, T. *J. Biomed. Mater. Res.* **1995**, *29*, 349.
(9) Zhang, S.; Gonsalves, K. E. *Mater. Sci. Eng.* **1995**, *C3*, 117.
(10) Zhang, S.; Gonsalves, K. E. *Langmuir* **1998**, *14*, 6761.
(11) Kato, T.; Suzuki, T.; Amamiya, T.; Irie, T.; Komiyama, M. *Supramol. Sci.* **1998**, *5*, 411.
(12) Iwatsubo, T.; Sumaru, K.; Kanamori, T.; Yamaguchi, T.; Shinbo, T. *J. Appl. Polym. Sci.* **2004**, *91*, 3627.
(13) Iwatsubo, T.; Kusumocahyo, S. P.; Kanamori, T.; Shinbo, T. *J. Appl. Polym. Sci.*, accepted for publication.
(14) Williamson, G. R.; Wright, B. *J. Polym. Sci., Part A* **1965**, *3*, 3885.
(15) Sikes, C. S.; Wheeler, A. P. *CHEMTECH* **1988**, 620.
(16) Kröger, N.; Bergsdorf, C.; Sumper, M. *EMBO J.* **1994**, *13* (19), 4676.
(17) Kröger, N.; Deutzmann, R.; Sumper, M. *Science* **1999**, *286*, 1129.
(18) Poulsen, N.; Sumper, M.; Kröger, N. *Proc. Natl. Acad. Sci U.S.A.* **2003**, *100*, 12075.
(19) Kuhn, P. W.; Hargitay, B.; Katchalsky, A.; Eisenberg, H. *Nature* **1950**, *165*, 514.
(20) Oyane, A.; Onuma, K.; Ito, A.; Kim, H.-M.; Kokubo, T.; Nakamura, T. *J. Biomed. Mater. Res.* **2002**, *64A* (2), 339.
(21) Ishidao, T.; Akagi, M.; Sugimoto, H.; Onoue, Y.; Iwai, Y.; Arai, Y. *Fluid Phase Equilib.* **1995**, *104*, 119.
(22) Iwatsubo, T.; Shinbo, T. *J. Macromol. Sci., Phys.* **2001**, *B40* (6), 1017.
(23) Nagasawa, M.; Izumi, M.; Kagawa, I. *J. Polym. Sci.* **1959**, *37*, 375.
(24) Luecke, H.; Quiocho, F. A. *Nature* **1990**, *347*, 402.
(25) Kagi, H.; Nagai, T.; Komatsu, K.; Okada, T.; Wada, C.; Loveday, J. S.; Parise, J. B. *J. Neutron Res.* **2005**, *13*, 21.
(26) Hecky, R. E.; Mopper, K.; Kilham, P.; Degens, E. T. *Mar. Biol.* **1973**, *19*, 323.

BM0504476